QUANTITATIVE X-RAY CT
FOR
SCAL PLUG HOMOGENEITY ASSESSMENT

Jos G. Maas and Albert Hebing
PanTerra Geoconsultants BV, The Netherlands

This paper was prepared for presentation at the International Symposium of the Society of Core Analysts held in Napa Valley, California, USA, 16-19 September, 2013

ABSTRACT

Heterogeneities in core plugs may dominate flow and provoke early water breakthrough in laboratory displacement experiments. Derived relative permeabilities would have been measured to provide input into reservoir simulation models but will then not be representative for the field. Unrepresentative heterogeneities in a core plug may so dominate the prediction of field performance. To prevent that, first the core, and subsequently the core plugs are X-ray CT scanned to assess heterogeneities. However, so far the industry does not have a quantitative tool: the CT images are judged from an arbitrary-grey-scale picture and the interpretation is highly subjective.

We have set out to develop a quantitative tool by correlating, through a theoretical model, the standard deviation of the Hounsfield values in the digital CT images with the standard deviation of the permeabilities. To verify the validity of the model, a mini-permeameter has been used. 95 plugs have been measured, with permeabilities from less than 1mD up to several Darcys. For each plug, two cross-sectional images have been obtained, at right angles to each other, along the length of the core plug. The standard deviation in the CT-images was determined over several regions of interest, to allow accounting for edge artefacts. The mini-permeameter readings were taken every 5 mm on the top and bottom faces of the plug and over four lines along the length of the core plug, amounting to typically 80 points per plug in total.

A correlation is presented with which we can now objectively link the variation in permeability of a core plug to the standard deviation in Hounsfield values in a cross-sectional CT image. Assuming a threshold for an acceptable variation in permeability, this correlation gives us an acceptable standard deviation in a digital CT image independent of the settings of the grey scale of the image.

INTRODUCTION

SCAL flow experiments are conducted on core material to measure relative permeabilities, capillary pressure and resistivity (I-Sw) data to feed reservoir simulation models that analyse and predict field behaviour. A local heterogeneity in a plug may easily dominate flow behaviour in that plug and distort the measurement results [1]. It is not uncommon that a high-permeable streak, local to the plug, prompts an inadvertent early water breakthrough. The corresponding relative permeabilities, when input in a reservoir model, would provoke similar early water breakthrough on the scale of the field. The problem is recognised in the industry, and core and core plugs are routinely scanned in an X-ray CT scanner to ensure the selection of homogeneous, representative core plugs for SCAL experiments [2]. However, so far the industry does not have a tool for an objective, quantitative interpretation of CT images to assess homogeneity. As an example, Fig. 1 shows an image of core plug that is seemingly quite homogeneous. In Fig. 2, the same core plug is shown, with a different setting of the grey-scale and now the plug appears to be highly heterogeneous. CT scanners, for medical purposes, have a range of pre-set scale-settings, different for different parts of a human body, based on medical experience, to present an image suitable for an objective analysis by medical staff. Such pre-settings are missing for SCAL plug scanning. Even if the CT-scan facility would send the images in so-called DICOM format [3] to the SCAL laboratory, so that a SCAL specialist can edit the grey-scale to assess homogeneity, the industry does not have objective criteria to set the grey-scale. It is important to realise that it is not uncommon that a CT facility will send the images as jpeg or tif files to the SCAL laboratory. In such cases, the digital information in the image is effectively frozen by the grey-scale, rendering the images useless for a homogeneity assessment.

To address this issue, we have set out to develop a quantitative tool by correlating the standard deviation of the so-called Hounsfield values in the digital CT images with the standard deviation of the permeabilities obtained with a mini-permeameter. We will first present a theoretical model that provides the basis for constructing a correlation. Subsequently, we discuss the experimental work conducted to verify the validity of the correlation.

THEORETICAL MODEL

Water flood performance in the field is long known to be dependent on reservoir heterogeneity, and more in particular on permeability variations in the field [4]. Similar to industry practice for assessing heterogeneity in the field [4] or recently in a micro-CT compaction study [5], we will use the coefficient of variation V of the absolute permeability as a quantitative measure of heterogeneity in a core plug:

$$V = \frac{\sigma_K}{\overline{K}} \qquad (1)$$

with σ_k the standard deviation of the absolute permeability K, measured locally at many points in the plug and $\overline{K}$ the absolute permeability averaged over those points. A mini-permeameter can only probe points along the surface of the plug, whereas an X-ray CT scanner produces images of the interior of a plug, but permeability in that case can only be assessed indirectly, in a two-step process.

Firstly, the digital information in a CT image is expressed in so-called Hounsfield units (HU) of X-ray absorption [6]:

$$HU = \left(\frac{\mu - \mu_w}{\mu_w - \mu_{air}}\right) * 1000 \qquad (2)$$

with μ the linear absorption coefficient of the material and μ_w, μ_{air} the linear absorption coefficient of water and air respectively. Assuming that the plug consists of a dry material with porosity φ, and linear absorption coefficient μ_r we have

$$\mu = (1 - \varphi)\mu_r \qquad (3)$$

Combining Eq. 2 and 3 shows that HU is a linear function of porosity. Fig. 3 demonstrates this relationship as determined for a number of plugs in the current study. Note the very high correlation coefficient squared R^2, which is very typical for such CT data.

The general form for this relationship is

$$HU(\varphi) = -a\varphi + b \qquad (4)$$

with *a* and *b* constants and positive.

Secondly, porosity is linked to permeability, using the relevant poro-perm relationship as measured in the laboratory as part of most routine core analysis programs. In many cases, the data on a permeability-porosity cross-plot can be reasonably well fitted by a straight line on a semi-log K - φ plot [7]. This can be translated into

$$K(\varphi) = ce^{d\varphi} \qquad (5)$$

with *c* and *d* constants and positive.

In order to link the coefficient of permeability variation V to the information in CT images, we consider the statistical distribution of the various parameters. Porosity on reservoir scale is believed to be normally (Gaussian) distributed [8], while permeability is assumed to be log-normally distributed [9]. We will assume that the same features hold on the scale of the core plugs. Note that the exponential function in Eq. 5 prescribes that a normally distributed porosity will generate a log-normal distribution in permeability [10], consistent with our assumption.

From statistics theory [10], and using Eqs. 4 and 5, we have that the standard deviation measured in CT Hounsfield values σ_{HU} is related to the underlying standard deviation σ_{lnK} of ln(K) as

$$\sigma_{lnK} = \left(\frac{d}{a}\right)\sigma_{HU} \qquad (6)$$

Also, from statistics theory, we have a relation between the standard deviation σ_{lnK} of ln(K) and the standard deviation σ_k of K as observed on a linear permeability scale [10, 11]:

$$\sigma_{lnK}{}^2 = \ln\{1 + \left(\frac{\sigma_K}{\overline{K}}\right)^2\} \qquad (7)$$

Combining Eqs. 1, 6 and 7 we have for permeability variation V<<1:

$$V = \frac{\sigma_K}{\overline{K}} \simeq \left(\frac{d}{a}\right)\sigma_{HU} \qquad (8)$$

So, with *a* and σ_{HU} measured from the digital CT images and *d* obtained from the experimentally observed poro-perm correlation, we can estimate the permeability variation V in a core plug. In this study, mini-permeability readings on the plugs were used to verify the validity of this correlation for V.

EXPERIMENTS

The study was conducted on 95 plugs, of 1.5” diameter and 3 to 5 cm length, with permeabilities ranging from below 1mD up to several Darcys. Porosities ranged between 0.02 and 0.5. Most plugs were taken from sandstone reservoirs (66 plugs, 7 reservoirs); 13 plugs from four chalk formations; 9 plugs from Oberkirchener sandstone outcrop and 7 test plugs of sintered glass were measured.

CT scans were taken preferably on plugs positioned vertically, with two scans in so-called tomogram-mode, longitudinally through the plug, at right angles with respect to each other (Fig. 4). The X-ray CT scanner was operated at 120 kV, 500mA, 2.5 mm slice thickness, with four images in one frame-set taken 2.5 mm apart for each “shot”. The mean Hounsfield value and standard deviation were obtained of each image, using several regions-of-interest (ROI’s) across the image to account for so-called beam-hardening effects[1]. These measurements were conducted with the free-ware software “Sante DICOM viewer free”. The grey-scale in the images is defined by two parameters: the window-centre (also called “level”, dependent on CT manufacturer) value that indicates the mid-point in HU for the scale, and the window-width value that indicates the

[1] Rectangular ROI’s were set across the images, with the sides parallel to the sides of the core plugs, each consecutive ROI smaller and fitting within the previous ROI. Readings of mean and HU and standard deviation were recorded when the ROI was some 5 mm away from the sides or when data differed less than some 5 HU, whichever came first.

span of CT values covered by the scale setting. Any values below the window will appear as black, and any values above the window will appear as white in the image.

For viewing the images, we used centre values close to the mean HU in the image, and a window-width of 200 HU.

Unsteady-state mini-permeameter data were obtained mostly at a grid spacing of 5 mm across top and bottom, and 5mm apart along 4 lines along the (curved) side of the plugs. Generally, around 80 readings were taken per plug. The mini-permeameter technology is based on the work by Jones [12]. The test probe had a "nose-tip" of 5 mm diameter (bound by an O-ring). Klinkenberg-corrected permeabilities were collected by an automated measurement system.

As part of the routine core analysis (RCA), ambient He porosity was measured through Boyle's law. In addition, Klinkenberg-corrected whole plug absolute permeability was determined by flowing with N_2, with the plug mounted in a Hassler-type core holder at a nominal confining pressure of 400 psi.

All CT and mini-permeameter measurements were conducted at zero overburden.

RESULTS

X-Ray CT images

As indicated above, for all plugs Eq. 4 was fitted to the mean HU values of the CT images and the factor *a* was determined, similar to what is shown in Fig. 1. R^2's were usually above 0.9, so *a* was accurately established. The outcrop samples and the sintered glass samples presented a problem, because the spread in porosity for these samples was too small for a reliable correlation to be established for the mean HU values. In these cases, we used a fit in line with the average values we found in the other samples and in literature [13].

It is of interest to note that standard CT DICOM image format allows HU values between -1024 and +3071 [3]. We observed that some samples showed HU values of 3071 within an ROI, suggesting that actually higher CT numbers could have occurred. For those samples, a special scanner option for an extended scale setting could be used that effectively multiplies the minimum and maximum displayable CT numbers by a factor of 10. Indeed, these samples showed then values of 5000 and more, indicative of the presence of pyrite [13] or other strong X-ray absorbing materials[2].

Permeability measurements

RCA poro-perm data were used to obtain the factor *d* after fitting the data to Eq. 5. R^2's were now between 0.6 and 0.8 and in one case only 0.3 (see Fig. 5). Again for the outcrop and sintered glass samples the porosity spread was too limited to establish a correlation. For these samples, we used a fit of Eq.5 to the Kozeny-Carman equation for the porosity

[2] Thin section analysis proved the presence of barite and siderite patches in these samples.

range of interest. We found that for a porosity range limited to some 5 porosity units around any centre value, an excellent fit was obtained with Eq. 5, with the factor *d* dependent on the centre-value under consideration.

The miniperm data were averaged and compared to RCA whole plug Klinkenberg-corrected permeability data as a quality check. All reservoirs showed good cross-correlations (e.g. data in Fig. 6), except one. The samples of this reservoir happened to be the only samples that had been drilled vertically. Moreover, these samples showed on CT some clear layering and generally a large spread in top-bottom absolute permeabilities, so large V-values.

Finally, it was observed that for many plugs the standard deviation of the miniperm readings on the four lines along the curved side was significantly larger than for top or bottom readings. Two effects are likely to be contributing:

- For these horizontally drilled plugs, the permeability probed along the curved sides may correspond to horizontal permeability, vertical permeability, or a mix between these, dependent on the rotation of the plug along its axis. This is likely to result in readings showing lower permeability than the horizontal RCA data.
- We noticed that the miniperm probe had difficulty in sealing on a round surface, even with the radius of curvature reasonably large (all plugs were 1.5" diameter) and the probe tip rather small (5mm diameter): alignment of the plugs with the travelling probe proved tedious and was not always perfect, resulting in occasional high readings.

Correlation results

As an example, Figs. 7 and 8 show a detailed comparison between the permeability variations V as measured with the miniperm and as predicted with the correlation, using the information in the CT images and the poro-perm relationship from RCA for the 9 outcrop samples and the 13 Chalk samples. The correlation appears to work well, except for outcrop sample 8.

An overview of the results for all horizontal plugs (including the outcrop and chalk plugs) is presented in Fig. 9 that shows a comparison between predicted permeability variation V, based on Eq. 7, along the horizontal axis and the actually observed miniperm variation, along the vertical axis. To arrive at the plot in Fig. 9,

- We have discarded the miniperm data measured along four lines on the curved side of the plugs, since we deemed these to be not representative, as discussed previously.
- We have applied a cut-off of 0.35 to the relative porosity variation. The procedure to estimate this variation and the rationale for the cut-off is discussed in the next section.

For one reservoir, 17 samples were drilled vertically, perpendicular to the bedding plane. We could not correlate the measured permeability variation for these samples with our model. The average permeability variation measured with the miniperm was 0.9, while the average predicted variation amounted to 7.

Finally, as a general observation, we noticed that visual inspection of any sample proved to be highly unreliable in assessing homogeneity.

DISCUSSION

The quality of the correlation is analysed by interpreting R^2 of the straight line fitted through the data and forced to cross through (0,0) in Fig. 9. By taking the square root of R^2, we arrive at the ("Pearson") correlation coefficient proper, being in this case 0.56. The number of samples that made the cut-off amounts to 62. From standard statistical tables, we conclude that there is a probability of more than 99% that the derived correlation is significant for this sample set. With the slope very close to unity, we have an excellent correspondence between the theoretical model and the mini-permeameter data.

The theoretical model is based on assumptions that need to be verified for each sample-set it is applied to. The first assumption is that porosity follows a normal (Gaussian) distribution. This assumption may be violated at large σ_{HU}: the standard deviation σ_φ of the porosity distribution is equal to σ_{HU}/a (see Eq. 4), so for any data with σ_{HU}/a close to, or even larger, than the mean porosity in the sample, the porosity distribution is likely to be non-Gaussian. We found that for σ_φ/φ larger than 0.35, the correlation between predicted and measured permeability variation broke down.

A second assumption is the validity of Eq. 5 for a sample set. A low value of the correlation coefficient when fitting Eq. 5 may bring about a low validity of the correlation for the permeability variation if the sample set is too small (to be assessed using a Pearson table). Given the high correlation coefficients found for the CT data (Eq. 4), the correlation coefficient for the poro-perm relationship is likely to be dominating the validity of the correlation for the permeability variation.

Another assumption is that the value measured for σ_{HU} within an ROI is representative for the sample. This turned out to be the issue with outcrop sample 8 in Fig. 7, mentioned above. Upon re-examining the local permeability variation of this sample, we found that the observed large V, averaged over top and bottom, was caused by a permeability at the top of the sample being significantly different (factor 3 or more) than the permeability at the bottom. The standard deviation in permeability observed at the top and at the bottom of the plugs individually was small. Upon re-examining the CT-images, it became clear that the porosity indeed varied significantly, but only very close to the edge of either the top or the bottom of the plug[3]. So, this heterogeneity could only be analysed

---

[3] To study this in more detail, thin sections were taken from top and bottom of plug 8 and compared. The point count results showed indeed that the sandstone in the upper part of the plug contains more kaolinite and more pore space than the lower part.

quantitatively through a small ROI near either the top of the bottom. Over a large ROI, the local disturbance averaged out and disappeared into overall standard deviation.

However, exactly near the edges, the HU values in the images are impacted most by beam-hardening, and a so-called cupping effect is noticeable [14]. This cupping effect may also artificially increase the measured σ_{HU}, which we found to be another error source that may limit the accuracy of the correlation. Actually, the cupping effect is clearly seen both in Figs. 1 and 2: it shows up as the white lining around the samples.

We note that several other samples show predicted permeability variations smaller by a factor 3 than the values actually observed with the miniperm. These samples all had local permeability distortions similar to what was discussed above for the outcrop sample 8. Another anomaly is that some samples showed predicted permeability variations larger by a factor 4 or more than the values actually observed with the miniperm. These samples all showed a σ_{HU} of several 100's (up to 750) in combination with observed values for V of some 0.4 to 0.6. Upon re-examining the CT-images of these samples, we noticed that the images had many spots with high CT values over 3071, homogeneously spread over the ROI's. Given the set-up of our correlation, apparently the large σ_{HU} for these samples does not correspond to a large spread in porosity, but just indicates a large spread in X-ray absorption characteristics.

Within the limitations mentioned above, we have now a correlation to estimate permeability variation V combining image analysis of cross-sectional tomograms and poro-perm data from RCA on core plugs. Once that we select a value for V deemed acceptable for SCAL flow experiments, we can derive immediately the corresponding limit on σ_{HU} in the CT images. As a practical example, we list in Table 1 the maximum allowable σ_{HU} as a function of chosen acceptable values of V for (sandstone) sample set B and for 10 chalk samples.

To select an acceptable V, we need to realise that statistically some 68% of the permeabilities locally in a core plug will be found between $(\overline{K} - \sigma_K)$ and$(\overline{K} + \sigma_K)$, and about 96% between $(\overline{K} - 2\sigma_K)$ and $(\overline{K} + 2\sigma_K)$.

CONCLUSIONS AND RECOMMENDATIONS

- A correlation has been established to objectively assess core plug homogeneity for a given acceptable permeability variation V, using statistical information in DICOM-formatted CT images and the poro-perm data established in RCA.
- The standard deviation in HU units is then used for screening the samples.
- We recommend setting the grey-scale window-centre close to the mean HU value and the window-width to 200 HU. In our experience, this allows a quick pre-screening of the samples because significant heterogeneities could already then be highlighted.

- Visual inspection of just the core plugs, without CT imaging, is highly unreliable in detecting heterogeneities. However, plugs that have visually detectable layering or other features can already be flagged as of questionable homogeneity.
- We recommend to first CT-scan whole core using a topogram[4], to assess the best locations to drill SCAL plugs. Then CT scanning in tomogram mode should be conducted on cleaned and dry plugs: fluid content will interfere with the HU profile in the images[5]. In case topograms cannot easily be obtained on whole core, an alternative approach would be to drill many more SCAL plugs than required for the measurement program, to allow a significant fraction to be disqualified later, based on too large heterogeneities found in the CT images of the plugs. In our experience, more than half of the samples drilled without pre-screening by topograms may need to be discarded later.
- Beam hardening remains an issue, and may limit the accuracy of the correlation. We recommend using rock-specific beam-hardening corrections. This may not be possible with most modern medical CT scanners, but there may be options using a micro-CT scanner in low resolution mode. Another option is using pre-hardening shells around the plugs [15].
- The accuracy of the correlation is likely to be limited mainly by the reliability of the fit of the poro-perm correlation; the data in the Hounsfield plot are usually fitted with correlation coefficients close to unity.
- The correlation could not be validated for vertical samples with horizontal layering.

ACKNOWLEDGEMENTS

We gratefully acknowledge that many CT scans were supplied courtesy of Karl-Heinz Wolf and Wim Verwaal, Technical University Delft (TUD). Ellen Meijvogel TUD, who conducted the CT scans, provided us also with expert advice on CT protocols. Technical support around the mini-permeameter was in the good hands of Michael Casey and Daniël Sierat. We thank Niels Springer (GEUS) for supplying us with chalk core plug samples, including the relevant RCA and CT data and for his insightful comments on the statistical analysis.

REFERENCES

1. Zweers, A., W. Scherpenisse, K. Wit and J. Maas, “Relative Permeability Measurements on Heterogeneous Samples- A pragmatic approach”, SCA-9909 (1999).

2. Midtlyng, S. H. and J. Å. Stensen, “Improved flooding experiments in heterogeneous rocks using in-situ saturations from X-ray CT measurements”, SCA2000-40 (2000).

---

[4] Note that a topogram (X-ray projection image) generally does not show calibrated Hounsfield values.

[5] The difference between dry porous rock and liquid filled rock may be 100 to 200 HU’s, dependent on porosity.

3. DICOM is a medical image formatting standard. The DICOM CT format allows for 12-bit storage of integers, limiting the HU scale to values between zero and 4095, while vacuum would need to show as -1000. Therefore, an offset is applied of 1024 to correct for this, limiting the maximum displayed HU value to 3071.

4. Craig, F.F., Jr., "The reservoir engineering aspects of water flooding", Vol. 3 of the Henry L. Doherty. Series, SPE, New York (1971).

5. Louis, L., P. Baud, A. Rolland and T.-f. Wong, "Compaction localization in high porosity sandstones with various degrees of heterogeneity: insight from X-ray computed tomography", Proceedings of the 3rd CANUS Rock Mechanics Symposium, Toronto, May 2009 (Ed: M. Diederichs and G. Grasselli), abstract 1143, 1-2.

6. Hounsfield, G.N., "Computed Medical Imaging Nobel Lecture, 8 December 1979", J Radiol. (1980) **61,** 6-7, 459-68.

7. Tiab, D., and E. C. Donaldson, "Petrophysics: Theory and Practice of Measuring Rock and Fluid Transport Properties", Gulf Publishing Co, Houston (1996).

8. Harrop-Williams, K., "Random Nature of Soil Porosity and Related Properties" , J Eng. Mech. (1989) **115**, 5, 1129-1133.

9. Dullien F., "Porous Media: fluid transport and pore structure", Academic Press, New York (1991), 139-176.

10. Weisstein, Eric W., "Log Normal Distribution", from MathWorld--A Wolfram Web Resource, http://mathworld.wolfram.com/LogNormalDistribution.html (2013).

11. Limpert, E., W.A. Stahel and M. Abbt, "Log-normal Distributions across the Sciences: Keys and Clues", Bioscience (2001) **51**, 5, 341-352.

12. Jones, S.C., "The Profile Permeameter - A New, Fast, Accurate Minipermeameter", SPE 24757 (1992).

13. You, S. and H.G. Ji, "Characterisation by X-ray computed tomography of the bedding planes influence on excavation damaged zone of a plastic clay" in "Rock Mechanics: Achievements and Ambitions", Cai (ed.), Taylor and Francis Group, London (2012), 245-248.

14. Da Costa e Silva, A., "Analysis of viscous fingering reproducibility in consolidated natural porous media", SCA-9504 (1995).

15. Coles, M.E., E. L. Muegge and B. F. Marek, "Use of attenuation standards for CAT scanning applications within oil and gas production research", SCA-9223 (1992).

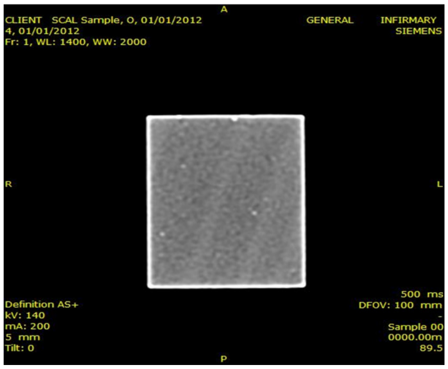

Fig. 1. CT image of typical sample appears to be homogeneous.

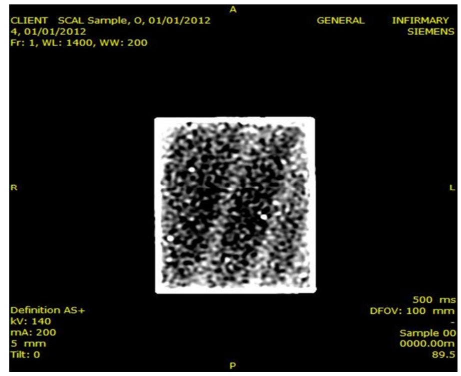

Fig. 2. CT image of same sample as in fig.1, but with different grey-scale setting, now appears to be heterogeneous.

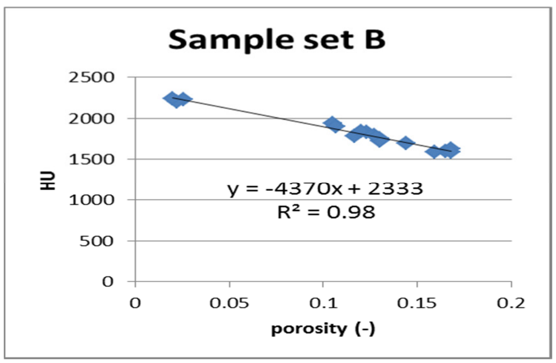

Fig. 3. Measured Hounsfield values for samples in set B. Excellent correlation is observed with a straight line as function of porosity.

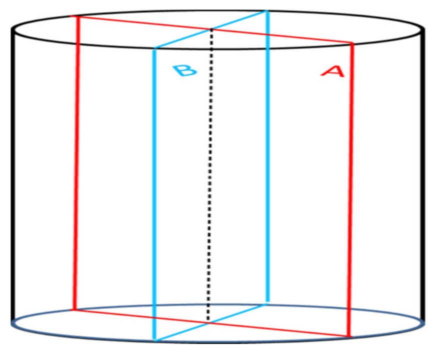

Fig. 4. Positioning of tomograms A and B taken longitudinally through a core-plug mounted vertically.

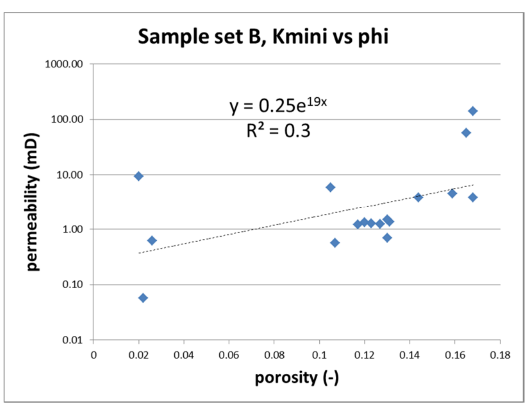

Fig. 5. Poro-perm relationship for sample set B.

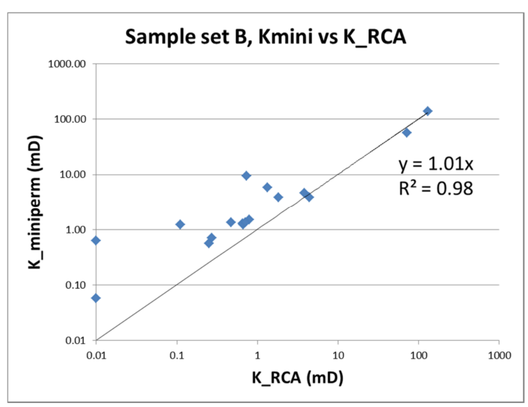

Fig. 6. Comparison of mini permeameter data with RCA permeability for set B.

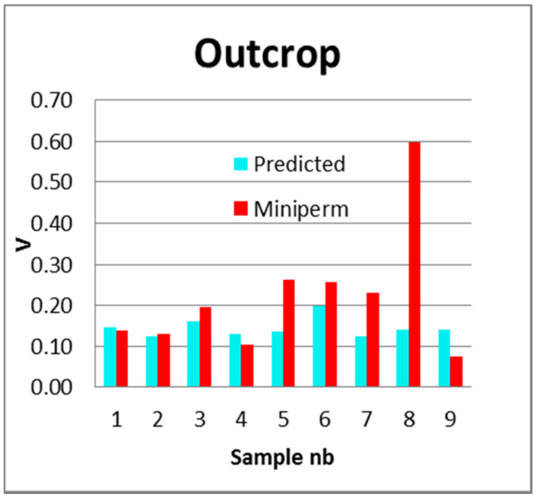

Fig. 7. Permeability variation V, comparison between predicted with correlation and measured with miniperm on sandstone outcrop samples. Sample 8 proved to have local distortion close to the bottom edge, not picked-up with CT analysis.

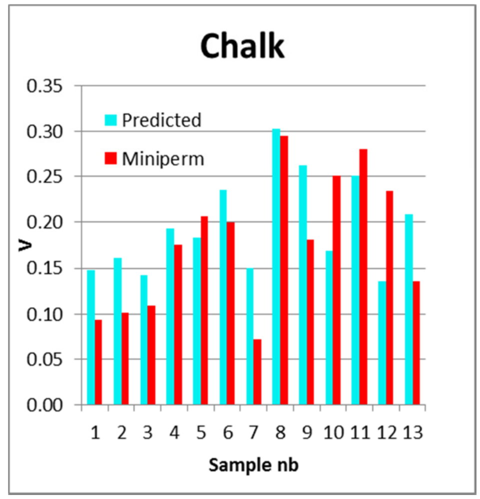

Fig. 8. Permeability variation V, comparison between predicted with correlation and measured with miniperm on chalk samples.

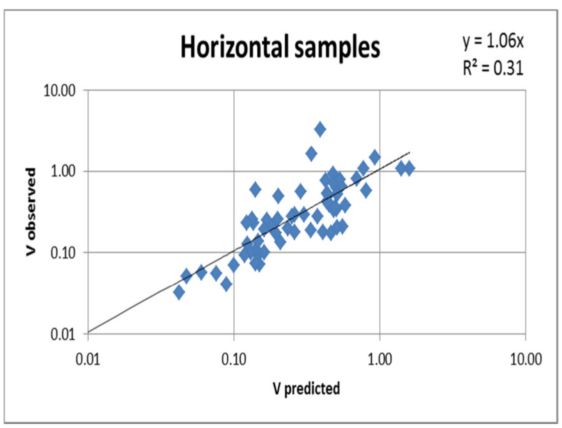

Fig. 9. Permeability variation V as measured with miniperm vs. V predicted with correlation on all horizontal samples, excluding samples with relative standard deviation in porosity larger than 0.35

V	Sample set B (sandstone) Max σ_{HU}	10 chalk samples Max σ_{HU}
0.05	12	18
.1	25	35
.2	45	70
.3	70	105

Table 1. Maximum allowable σ_{HU} in CT images for (sandstone) sample set B and 10 chalk samples, as a function of various assumed acceptable values of the permeability variation V.